IMMUNOBIOLOGY

Lymph node B lymphocyte trafficking is constrained by anatomy and highly dependent upon chemoattractant desensitization

*Chung Park,[1] *Il-Young Hwang,[1] Rajesh K. Sinha,[1] Olena Kamenyeva,[1] Michael D. Davis,[1] and John H. Kehrl[1]

[1]B-Cell Molecular Immunology Section, Laboratory of Immunoregulation, National Institute of Allergy and Infectious Diseases, National Institutes of Health, Bethesda, MD

B lymphocyte recirculation through lymph nodes (LNs) requires crossing endothelial barriers and chemoattractant-triggered cell migration. Here we show how LN anatomy and chemoattractant receptor signaling organize B lymphocyte LN trafficking. Blood-borne B cells predominately used CCR7 signaling to adhere to high endothelial venules (HEVs). New B cell emigrants slowly transited the HEV perivenule space, and thereafter localized nearby, avoiding the follicle. Eventually, the newly arrived B cells entered the basal portion of the follicle gradually populating it. In contrast, newly arriving activated B cells rapidly crossed HEVs and migrated toward the lymph node follicle. During their LN residency, recirculating B cells reacquired their sphingosine-1 phospate receptor 1 (S1P1) receptors and markedly attenuated their sensitivity to chemokines. Eventually, the B cells exited the LN follicle by entering the cortical lymphatics or returning to the paracortical cords. Upon entering the lymph, the B cells lost their polarity, down-regulated their S1P1 receptors, and subsequently strongly up-regulated their sensitivity to chemokines. These results are summarized in a model of homeostatic trafficking of B cells through LNs. (*Blood*. 2012;119(4):978-989)

Introduction

Lymphocyte homeostasis in resting lymph nodes (LNs) is maintained by the entry of circulating lymphocytes through high endothelial venules (HEVs) and exit through lymphatic vessels. CD62L on lymphocytes interacts with ligands on HEVs in LNs to initiate the rolling of lymphocytes along the luminal surface.[1,2] As the lymphocytes roll, cognate G-protein coupled receptors (GPCRs) engage homeostatic chemokines present on the luminal surface of HEVs triggering lymphocyte adhesion and the exploration for a transendothelial migration (TEM) site.[3] After penetrating the endothelial basement membrane, the cells negotiate the perivenule space to emerge in the paracortical cords (PCCs).[4-6] These cords originate between and below LN follicles and extend to the medullary region of the LNs where they merge with the medullary cords. After crossing the HEVs, the migratory paths of B and T lymphocytes diverge. T cells migrate along CCL19/21 expressing fibroreticular cells (FRCs) using their prominently expressed CCR7 to access the LN deep cortex whereas B cells rely on their prominent CXCR5 expression to access the LN follicle.[7-9] Newly resident B cells tend toward the follicle centers, sites of high CXCL13 expression, whereas long-term LN follicle residents move toward the edges closer to egress sites.[10] To enter the efferent lymph in route to the blood, B cells must leave the LN follicle, and eventually traverse the efferent lymphatic endothelium.

Although the high concentration of chemokines in the LN opposes lymphocyte LN egress,[11] another GPCR the sphingosine-1 phosphate receptor 1 (S1P1 receptor) has been implicated in facilitating lymphocyte egress into the lymph.[12-14] The LN parenchyma, although rich in homeostatic chemokines, has little S1P whereas the lymph and blood have high levels. A delicate balance between the synthesis, transport, and degradation of S1P achieves and maintains this gradient.[15] An explosion of interest in S1P signaling followed the observation that the administration of a S1P analog FTY720 caused lymphopenia by preventing lymphocyte LN egress.[12] Despite intensive scrutiny, a consensus on the mechanism by which FTY720 causes lymphocyte retention hasn't emerged.[13,16] However, a recent study has implicated lymphocyte S1P1 receptor cell-surface residency as a crucial factor in lymphocyte egress kinetics after FTY720 treatment.[17] Less controversy surrounds the concept that the lymphocyte S1P1 receptor functions to facilitate normal lymphocyte LN egress, although the precise mechanism by which it does so remains unresolved.[10,18]

In this study, we used a combination of immunohistochemistry, intravital microscopy, and in vitro chemotaxis assays to study the trafficking of B cells through the inguinal LNs of mice. Based on our results, we offer a model of homeostatic B-cell trafficking through LNs.

Methods

Mice and cells

C57BL/6, B6.129P2(C)-Ccr7[tm1Rfor/J−], and B6.SJL-Ptprc[a] Pepc[b]/BoyJ mice were obtained from The Jackson Laboratory. *Gnai2^{−/−}* mice[19] were provided by Dr Lutz Birnbaumer, and backcrossed 8 times to C57BL/6. All animal experiments and protocols were approved by the National Institute of Allergy and Infectious Diseases Animal Care and Use Committee (ACUC) at the National Institutes of Health. Spleen and LN B cells were isolated by negative depletion as previously described.[10] In some instances LN and blood B cells were isolated by FACS, sorting B220^{+}CD19^{+} cells using a FACS Aria (BD Biosciences). SVEC4-10 cells (CRL-2181) were from ATCC.

Reagents

D-erythro-sphingosine 1-phosphate and W146 were purchased from Avanti Polar Lipids. FTY720 was supplied by Dr Volker Brinkmann (Novartis Pharmaceutical). Murine CXCL13, CCL19, and CXCL12 were purchased from R&D Systems. Fatty-acid free bovine serum albumin (FAF-BSA) was purchased from Sigma-Aldrich. Antibodies and flow cytometry reagents used were as follows: antibody to S1P1 receptor (Santa Cruz Biotechnology); CD62L (BD Biosciences); LYVE-1 and phycoerythrin (PE) conjugated donkey anti–rabbit IgG (R&D Systems); anti–goat IgG-Rhodamine Red-X, anti–rabbit IgG-Rhodamine Red-X, streptavidin-Rhodamine Red-X, and normal donkey serum (Jackson ImmunoResearch); biotin-conjugated anti-CCR7 (BioLegend); anti-CXCR4, anti-CXCR5, anti-CD62L, allophycocyanin (APC)–conjugated anti-B220, PerCP-Cy5.5–conjugated anti-B200, and PE-conjugated anti-B220 (BD Pharmingen), Streptavidin-phycoerythrin, Streptavidin-efluor 450, and efluor 450–conjugated anti-B220 were from eBioscience.

Changes in $[Ca^{2+}]_i$, chemotaxis, and transmigration

Cells were seeded at 10^5 cells per 100 μL loading medium (RPMI 1640, 10% FBS) into poly-d-lysine coated 96-well plates (Nalgene Nunc). An equal volume of loading buffer (FLIPR Calcium 3 assay kit, Molecular Devices) was added. Cells were incubated for 1 hour at 37°C before adding chemokine, and then the calcium flux peak was measured using a FlexStation 3 (Molecular Devices). Data are shown as fluorescent counts and the y-axis labeled as Lm1. Chemotaxis assays[10] and transendothelial migration assays[20] were performed as previously described.

RT-PCR

RNA was isolated with the TRIZOL Reagent (Invitrogen) according to the manufacturer's instructions. Complementary DNA (cDNA) was synthesized from 1 μg RNA with Omniscript RT Kit (QIAGEN) with Omniscript reverse transcriptase. Standard primer pair sets were used. Real-time PCR was performed using a 7500 Real-Time PCR System (Applied Biosystems) following the Rotor-Gene SYBR Green PCR kit (QIAGEN) protocol. Relative gene expression = $2^{-\Delta\Delta Ct}$, where $\Delta\Delta Ct = (Ct_{gene} - Ct_{\beta-actin})$ CD62L mAb-treated LN B cell $- (Ct_{gene} - Ct_{\beta-actin})$ PBS-treated LN B cell.

Intravital two-photon laser scanning microscopy

Intravital two-photon laser scanning microscopy (TP-LSM) was performed with a Leica SP5 inverted 5 channel confocal microscope (Leica Microsystems) equipped with 20× multi-immersion objective, 0.7 NA as described.[10] Imaris Version 7.2.0 software was used to calculate cell velocity, speed variability and displacement. To outline microvessels 15 μL of Qdot solution (Qtracker 705) in 100 μL of PBS was injected into orbital or tail vein. To outline the lymphatics 3 μL of Qdot solution in 25 μL of PBS was injected into the tail base. To outline the lymphatic endothelium LYVE-1 antibody (R&D Systems, Clone: 223322) with Alexa Fluor 594 (10 μg) was injected subcutaneously close to the inguinal lymph nodes the day before imaging. Off-line analysis of cell behavior in microvessels was performed using Imaris Version 7.2.0 software as described.[21] The sticking fraction was the percentage of rolling lymphocytes that firmly adhered for at least 30 seconds. The intraluminal velocity and path length before transmigration were calculated from the Imaris tracking data. Transmigration was defined to begin when the cell stopped moving and began to leave the vessel lumen. The TEM duration was defined as the time from TEM initiation until the cell crossed to the perivenule space, which was outlined by previously transmigrated B cells. Blocking of the entrance and exit of B cells from the LN was done as previously described.[10]

Intracellular staining and flow cytometry analysis

The cells were intracellular stained using the BD Biosciences Cytofix/Cytoperm Fixation/Permeabilization Kit protocol using the S1P1 receptor antibody (dilution of 1:100), followed by the secondary donkey anti–rabbit IgG PE conjugated. The cells were resuspended with 1X BD Biosciences Perm/Wash buffer. All flow cytometry data were collected on a BD Biosciences FACS CANTO II or LSR II and analyzed with FlowJo Version 8.8.6 software (TreeStar).

Immunohistochemistry and immunocytochemistry

Freshly isolated LNs were snap frozen in Tissue-Tek OCT compound (Sakura Finetek). Six μm frozen sections were stained using standard techniques. For immunocytochemistry, lymph node and blood cells were immunostained with directly conjugated antibodies, methanol fixed, and immunostained for S1P1. In some instances, donor (CD45.2+) splenic B lymphocytes were adoptively transferred to recipient mice (CD45.1+). After 2 hours, some of the mice received 100 μg of CD62L antibody via tail vein injection. Either 2 or 16 hours after antibody injection, mice were killed and organs harvested for immunohistochemistry and flow cytometry to verify the transfer. The sections were immunostained for S1P1 receptor and CD45.2.

Statistics

In vivo results represent samples from 3 to 10 mice per experiment. In vitro results represent mean values of quadruplicate or sextuplet samples. SD and *P* values were calculated with the Mann-Whitney test or ANOVA using Microsoft Excel 2007 or GraphPad Version 5 Prism software.

Results

B cells cross HEVs slower than T cells and persist within the perivenule space

We used TP-LSM combined with fluorescent nanodots injected into the circulation to analyze the behavior of B cells in HEVs. Although our image acquisition rate (3/s) was too slow to measure rolling velocities, it was sufficient to examine the adherent cells. One day before imaging, we transferred labeled B cells to delineate the LN follicles. The following day we injected fluorescent nanodots into the recipient mouse to outline the LN vasculature, and transferred differentially labeled B cells. Within minutes, the B cells adhered to HEVs (Figure 1A). A lower percentage of the rolling B cells (17%) firmly adhered than T cells (Figure 1B; supplemental Figure 1A, available on the *Blood* Web site; see the Supplemental Materials link at the top of the online article). This probably reflects their lower expression of CCR7 and CD62L.[22,23] The majority of newly adherent B cells appeared within 70 minutes of transfer (Figure 1B). Initially, the adherent B cells had a typical spherical morphology; however, the cell rapidly flattened and polarized. Some cells quickly found permissive sites for TEM, others took several minutes, and some failed (supplemental Video 1). Approximately 60% of the cells that firmly adhered had transmigrated (data not shown). T cells out-competed B cells in the smaller HEVs, whereas in the larger HEVs the ratio was similar (supplemental Figure 1A). The smaller HEVs predominate in the cortical ridge and intrafollicular regions, whereas the larger HEVs reside closer to the LN medullary region. The average intraluminal velocity and path length between the site of firm adherence and TEM for B cells were 4 μm/min and 7 μm, respectively, whereas for T cells they were 9 μm/min and 6 μm, respectively (supplemental Figure 1B). The rate at which B cells transmigrated was significantly slower than that of T cells (supplemental Figure 1C, supplemental Video 2). This was independent of the fluorescent dyes used (data not shown). To pass through the initial barrier, the migrating B cells adopted an hourglass-like morphology (Figure 1C). After the initial passage, many cells remained flattened along the abluminal surface of the HEV, restricted from moving parallel
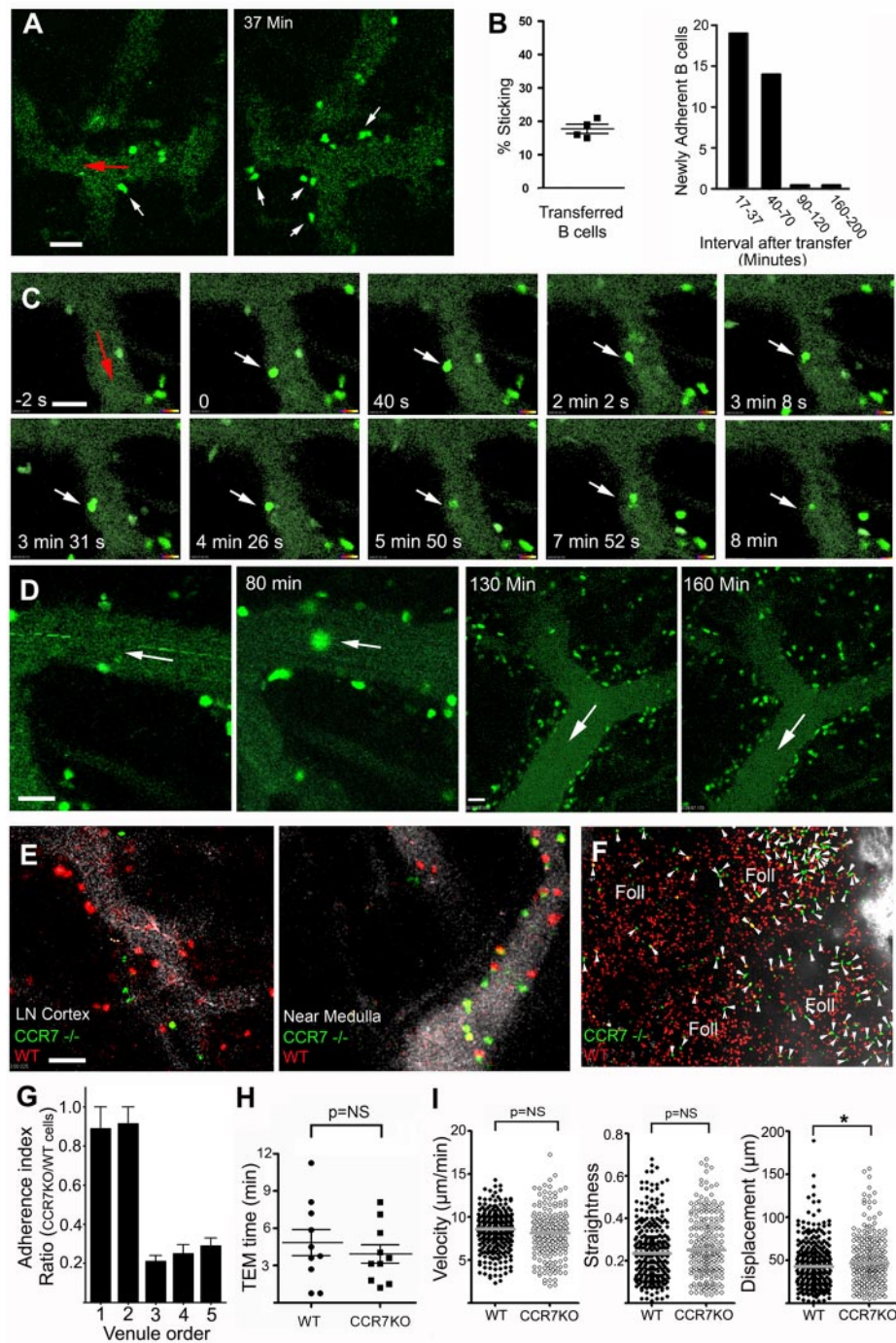
Figure 1. Entrance of B cells through LN HEVs. (A) Firm adhesion of transferred B cells. Two images acquired by TP-LSM at 17 and 37 minutes after adoptive B-cell transfer. HEVs outlined by fluorescent nanodots. White arrows indicate transmigrating cells and red arrow direction of blood flow. (B) B cells adhere to the endothelium. The percentage of rolling B cells observed to adhere in 4 separate experiments (left panel) over a 10-minute imaging interval. The number of newly adherent B cells that persisted for at least a minute noted over the indicated time intervals in a single HEV outlined by fluorescent nanodots (similar results in 3 other experiments, right panel). (C) Transmigration of a B cell. Individual images from TP-LSM that illustrate the transmigration of fluorescently labeled B cell (white arrows). Direction of blood indicated with a red arrow. Time is from the initial adhesion. (D) Prolonged association of B cells with HEVs. Individual images from TP-LSM of HEVs revealed by fluorescent nanodots showing transferred B cells at 30 and 80 minutes after transfer in the same HEV, and at 130 and 160 minutes after transfer in another HEV. White arrows show direction of blood flow. (E) Differential usage of HEVs by wild-type and $Ccr7^{-/-}$ B cells. Different HEVs, 1 in the LN cortex (left image) and 1 located near the LN medulla (right image). HEVs revealed by fluorescent nanodots before adoptive transfer of wild-type (red) and 3 times as many $Ccr7^{-/-}$ (green) B cells. Images acquired by TP-LSM. (F) Differential localization of wild-type and $Ccr7^{-/-}$ B cells in the LN. Equal numbers of wild-type and $Ccr7^{-/-}$ B cells were transferred 24 hours before TP-LSM. The location of the medullary region was identified by injection of an LYVE-1 antibody to outline its strong lymphatic staining. Four LN follicles (Foll) are present in the image. Arrowheads indicate $Ccr7^{-/-}$ B cells. Scale bars are 30 μm. (G) Ratio of adherent wild-type B cells to $Ccr7^{-/-}$ B cell on HEVs fractionated by vessel diameter. Venule order 1 through 5 are: > 50 μm, 40-50 μm, 30-40 μm, 20- 30 μm, and < 20 μm, respectively. (H) Transmigration of adherent wild-type and $Ccr7^{-/-}$ B cells. Time for TEM of individual cells measured between images acquired 5 to 35 minutes after transfer. No significant difference in the TEM times was found. (I) Velocity, straightness, and displacement of wild-type and $Ccr7^{-/-}$ B cells were analyzed using images 3 to 4 hours after transfer (*$P < .05$).
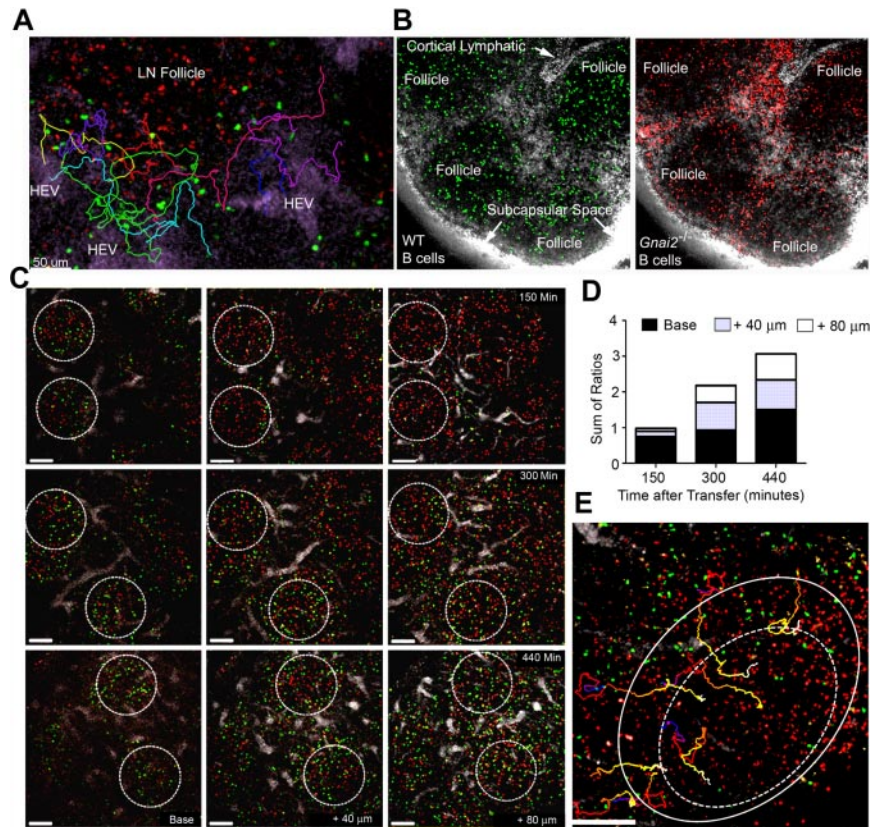
Figure 2. Entrance of B cells into LN follicles. (A) Recently arrived B cells avoid the LN follicle. Fluorescent nanodots were used to outline HEVs. Adoptively transferred B cells (green) were tracked between 40 minutes and 2 hours after transfer by TP-LSM in the vicinity of a LN follicle defined by labeled B cells (red) transferred 24 hours earlier. Individual tracks are shown in different colors. Images acquired every 15 seconds, 21 slices separated by 6 μm. (B) Many $Gnai2^{-/-}$ B cells fail to access the LN follicle. Wild-type (green) and $Gnai2^{-/-}$ (red) B cells were adoptively transferred 2 days before imaging. Red channel and green channel from the same image are shown. The lymphatics were outline by injecting labeled antibody against LYVE-1 (white) subcutaneously near the tail base. (C) B cells enter the LN follicle from the base. Three separate mice imaged at 150 minutes, 300, and 440 minutes after transfer of B cells (green). Follicles outlined with white circle based on the location of B cells (red) transferred the day before. Shown are images from 3 slices for each time period located at the base, at 40 microns, and 80 microns above the base. (D) Location of newly entering B cells in the LN follicle. The ratio of newly transferred to previously transferred B cells in base region, 40 microns, and 80 microns closer to the capsule is shown. The 3 ratios were summed. The results are from the analysis of imaging 8 follicles. (E) Tracking B cells entering the LN follicle. Newly-transferred B cells (green) were imaged by intravital TP-LSM for 1 hour starting at 3 hours 30 minutes after transfer every 15 seconds. For each time point, 21 slices were collected at 6 μm intervals. B cells (red) were transferred 24 hours before imaging to outline the follicle. Individual cell tracks are shown of B cells entering the LN follicle (outer circle) and crossing into the center region (dotted circle). Scale bars are 50 μm.

to the HEV, presumably located within the perivenule space. Curiously, many B cells persisted in this space for more than 1 hour (Figure 1D, supplemental Video 3).

$Ccr7^{-/-}$ B cells show a preference for large HEVs

Previous studies have indicated that both CCR7 and CXCR4 contribute to B lymphocyte homing to LNs.[22,23] To more carefully evaluate the behavior of $Ccr7^{-/-}$ B cells in HEVs, we transferred differentially labeled wild-type and $Ccr7^{-/-}$ B cells (3-fold more) into recipient mice. The ratio between wild-type and $Ccr7^{-/-}$ B cells adherent to HEVs varied according to the size of the HEV (Figure 1E). The $Ccr7^{-/-}$ B cells adhered better to the larger HEVs, and as a consequence, they preferentially localized in LN follicles located closer to the LN medullary region perhaps because they had used CXCR4 for entrance (Figure 1F). After adhering, the wild-type and $Ccr7^{-/-}$ B cells behaved similarly. Their TEM times were similar (Figure 1H), and 3-4 hours after transfer, they remained confined close to HEVs with similar track velocities and straightness, although the $Ccr7^{-/-}$ B cell tracks had a slightly greater displacement (Figure 1I, supplemental Video 4).

How B cells access LN follicles

Treating mice with CD62L Ab for 8 hours caused B cells near HEVs to disappear suggesting that newly arriving cells entered the LN follicle within that interval.[24] To more carefully delineate the kinetics and the path that newly entering B cells used to access the follicle, we transferred labeled B cells and imaged the area surrounding an HEV for various durations. As the B cells emerged from the perivenule space, they remained close to HEVs even at 3.5 hours after transfer (data not shown). Some cells approached the LN follicle, however they did not enter but veered away, often returning to the HEV area (Figure 2A, supplemental Video 5). This is very different from recent T-cell entrants, which rapidly accessed the T-cell zone. Between 1.5 and 2.2 hours after transfer, T cells can be observed in the T-cell zone, whereas B cells remained around the HEVs (supplemental Figure 1D, supplemental Video 6). Next, we verified the importance of chemoattractant receptor signaling for follicle access by comparing the LN localization of wild-type and $G\alpha_{i2}$ deficient B cells transferred 2 days previously. The loss of $G\alpha_{i2}$ (encoded by $Gnai2$) severely impairs B-cell chemotaxis.[25,26] Because they adhere poorly to HEVs, we adoptively transferred 3 times as many $Gnai2^{-/-}$ (red) as wild-type B cells (green). One
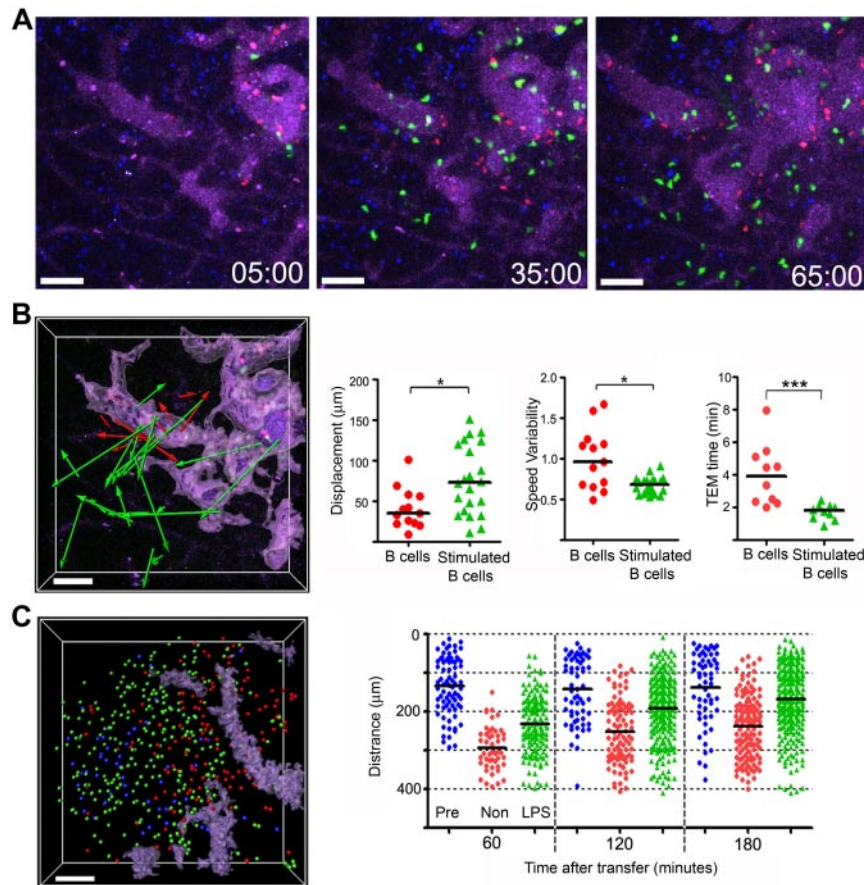
Figure 3. Stimulated B cells show distinctive behavior compared with that of nonstimulated B cells. (A) Still images acquired at the indicated time points from an hour intravital imaging shows the localization of adoptively transferred nonstimulated (red; CMTMR) or LPS-stimulated B cells (green; CMFDA). The dimension of LN follicle was visualized by previously transferred B cells (blue; CMAC) and HEVs were visualized with by the intravascular injection of quantum dot 705 (purple). The stimulated B cells were cultured overnight in the presence of LPS (1 μg/mL) and transferred simultaneously with freshly isolated B cells. (B) The image shows displacements of nonstimulated (red color arrows) or LPS-stimulated B cells (green color arrows) from the HEVs. The HEVs are highlighted (light purple) using the surfaces function in the Surpass view of Imaris. The tracks were randomly selected from tracks having durations greater than 10 minutes in an hour-long video. The individual tracks were analyzed to assess displacement and speed variability. Time for TEM of individual cells measured between images acquired 5 to 65 minutes after transfer (*$P < .05$; ***$P < .0001$). (C) Most LPS-stimulated B cells enter into B-cell follicles by 3 hours after transfer. The image shows the distribution of transferred B cells 3 hours after transfer. Pretransferred B cells (blue color spot) delineate the LN follicle. Locations of nonstimulated B cells (red), stimulated B cells (green) shown as colored balls. The HEVs are delineated by a light purple color. The graph shows the distance between each cell and a designated center of the LN follicle at various time points after cell transfer. The black bar is the mean value of each group. Scale bars are 50 μm. This experiment is representative of 3 performed.

hour before imaging, we injected labeled LYVE-1 antibody (white) near the inguinal LN to visualize the lymphatics (Figure 2B). In contrast to wild-type cells, many $Gnai2^{-/-}$ B cells remained outside the LN follicle in the interfollicular area and along the follicle edge, suggesting that Gα$_{i2}$-mediated signaling was needed for follicle access.

To determine how the newly arrived B cells entered LN follicles, we imaged at different depths within LNs based on the location of B cells transferred 24 hours earlier. We determined the ratio between newly arrived B cells and pretransferred B cells in the different regions as a function of time. At 150 minutes after transfer, some of the newly arrived B cells had entered the base of follicle. As time progressed, more cells entered the more superficial portions of the LN follicle (Figures 2C-D). Thus, newly arrived B cells accessed the follicle from its base close to the PCCs in the cortical ridge. Surprisingly, few B cells entered the LN follicle directly from the HEVs in the interfollicular region despite their close proximity to the follicle. Instead, these cells usually descended into the LN paracortex and often out of view. Eventually, B cells smoothly transitioned into the LN follicle (Figure 2E, supplemental Video 7).

Suggesting that B-cell activation might change how B cells traffic into the lymph node, we had noted that a day after transfer, LPS stimulated B cells moved faster and tended toward the follicle center[27] as do B cells that lack GPR183.[28,29] Here, we found that in contrast to nonstimulated B cells, the LPS stimulated cells rapidly emerged from the HEVs and by 1 hour after transfer many had moved away from HEVs (Figure 3A). The displacement of representative cells that exited from HEVs during the imaging period (Figure 3B left panel), along with the displacement and speed variability of the tracks (Figure 3B middle 2 panels) are shown. The stimulated B cells transmigrated more rapidly and upon escaping, the HEVs moved faster (Figure 3B right panel, data not shown). By 3 hours after transfer, many of the stimulated B cells had entered the follicle, whereas most of the nonstimulated cells remained near the HEVs. A snapshot of the locations of B cells transferred 24 hours earlier (blue), transferred 3 hours earlier (red), or stimulated and transferred 3 hours earlier (green) is shown (Figure 3C left panel). The distance from the center of the follicle of 3 groups of B cells is plotted for individual B cells at different time points (Figure 3C right panel).

B cells gradually reacquire S1P1 receptors after LN entrance

LN B cells will eventually exit the LN by crossing the lymphatic endothelium via an S1P1 receptor-dependent mechanism.[10] To assess B cell S1P1 receptor expression on recent entrants, we adoptively transferred CD45.2 B cells into CD45.1 mice. Two, 4, and 18 hours after transfer, LNs were harvested and then immunostained for CD45.2 and S1P1 receptor.[10,30] The mice from which we harvested the LNs at 18 hours received CD62L antibody to block the entrance of any additional B cells 2 hours after the adoptive transfer of B cells. At 2 hours, the transferred B cells were located close to HEVs and had low, but detectable S1P1 receptor expression (Figure 4A left panels). At 4 hours after transfer, the B cells were located either close to HEVs or in the cortical ridge region where their level of S1P1 receptor remained low (Figure 4A middle panels). By 18 hours after transfer, the majority of the B cells were located in the LN follicle. The transferred B cells had reacquired levels of S1P1 receptor similar to the surrounding follicular B cells (Figure 4A right panels). These data suggested that the levels of receptor expression would vary according to location of the B cells in the LN. Examination of B cell S1P1 receptor expression as a function of location in the LN confirmed this idea (Figure 4B-C). As expected, blood B cells had low levels of S1P1 receptors, whereas spleen and LN B cells expressed various levels (Figure 4D-E).

B cell chemokine receptor signaling desensitizes during LN residency

Decreased chemoattractant localizing signals within the LN would facilitate eventual B cell LN egress. Gradual desensitization of the signaling pathway during prolonged LN residency would provide a mechanism. To test that possibility, we compared LN B cells from mice treated 24 hours with CD62L antibody to those from controls. The average duration of B cell lymph node residency should be increased by the CD62L treatment as potential new entrants are prevented from crossing HEVs and those remaining would have entered at least 24 hours previously. Consistent with ongoing desensitization, LN B cells from CD62L-treated mice responded less well to chemoattractants than controls (Figure 5A). The antibody treatment should not affect splenic B-cell residency and accordingly spleen B cells from treated mice responded normally (Figure 5B). CD62L treatment not only impaired LN B cell chemotaxis, but also chemokine induced increases in intracellular Ca^{2+} (Figure 5C). However, chemokine receptor expression was unaltered (Figure 5D). Together these results indicate that receptor desensitization mediated by either receptor G-protein uncoupling or RGS protein induction had occurred.[31-33] Suggesting RGS protein involvement, RT-PCR documented increases in *Rgs1*, *Rgs3S*, and *Rgs16* mRNA in the CD62L antibody–treated group relative to control, whereas *Gnai2* and *Gnai3* expression levels remained constant. The differences in *Rgs* gene expression could not be accounted for by contaminating T cells or germinal center B cells (Figure 5E-F).

Although the treatment with CD62L provides a means to obtain B cells that have resided in LNs longer than those from nontreated mice, the continued egress of LN lymphocytes after CD62L treatment may alter the B cell population in additional and unknown ways. To provide another line of evidence that B cells desensitize their chemokine receptors during LN residence, we compared the chemotaxis of newly arrived B cells to the bulk population of the LNs and to those that had arrived later. By transferring CD45.2 B cells into CD45.1 mice, we could harvest

LNs at various durations after transfer and compare the endogenous and transferred LN B cells in the same assay. These experiments indicated that the more recently arrived B cells responded better to CXCL13 (supplemental Figure 2).

S1P1 receptor does not mediate LN B cell chemotaxis to S1P in vitro

An S1P gradient created by the diffusion of S1P from HEVs and lymphatics could provide a recruitment signal to facilitate B lymphocyte egress. However, splenic B cell S1P mediated chemotaxis is largely mediated by the S1P3, not the S1P1 receptor.[10] Immature B cells also use S1P3 receptors, not S1P1 receptors to migrate to S1P.[34,35] Similar to splenic B cells,[10] we found that S1P triggered LN B cells chemotaxis was not inhibited by a S1P1 receptor antagonist (supplemental Figure 3). To investigate how S1P might enhance the migration of B cells across the lymphatic endothelium, we used the mouse lymphatic endothelial line SVEC4-10.[20] We tested whether LN B cells would cross the inverted SVEC4-10 coated transwell inserts in response to S1P. However, very few cells did so. In contrast, CXCL13 supported LN B cell transmigration (supplemental Figure 3). To verify that S1P engaged the B cell S1P1 receptor, we showed that both S1P and pFTY720 induced S1P1 receptor endocytosis (supplemental Figure 3).

LN B cells enter the cortical lymphatics and rapidly depolarize

We previously imaged B cells in relation to the cortical lymphatic endothelium by infusing an antibody against LYVE-1.[10] However, this approach did not allow visualization of lymph flow. As an alternate approach, we injected fluorescent nanodots in the mouse tail region. The nanodots rapidly outlined the subcapsular sinus and quickly thereafter revealed the medullary and cortical lymphatics (Figure 6A, supplemental Video 8). Examination of the location of B cells adoptively transferred 18 hours earlier revealed that most resided within the LN follicle (79%), some were in the nearby PCCs and interfollicular region (16%), and a few were in the lymph (5%; Figure 6B). Within the lymph, the B cells rapidly lost their polarized phenotype reverting to a more spherical shape (Figure 6C-D). The velocity of cells in the PCCs was higher than the cells in the follicle (Figure 6E). Those cells that entered and remained within the cortical lymphatics tended to oscillate remaining largely stationary, whereas others entered and rapidly disappeared from view. If B cells only exited via the lymphatics adjacent to the LN follicle, then blocking entrance of cells through the HEVs should reduce the cells in the PCCs. However, numerous adoptively transferred B cells were visualized in the PCC 18 hours after administration of CD62L (Figure 6F left panels). Administration of FTY720 to block LN egress 6 hours before CD62L caused the PCCs to enlarge where the transferred B cells accumulated (Figure 6F right panels). Furthermore, a direct comparison of the same PCCs before or 5 hours after FTY720 revealed a 51% increase in the average PCC diameter ($P < .008$, paired t test). Directly imaging the inguinal LN from a CD62L-treated mouse at a different angle by gently turning the LN, showed B cells directly exiting the LN follicle into a PCC near the medullary region (Figure 6G). Imaging directly above the efferent lymphatic at the LN hilum revealed nonpolarized B cells flowing in the lymph (Figure 6H). Nonpolarized B cells and T cells can be seen exiting the lymph node (supplemental Video 9).
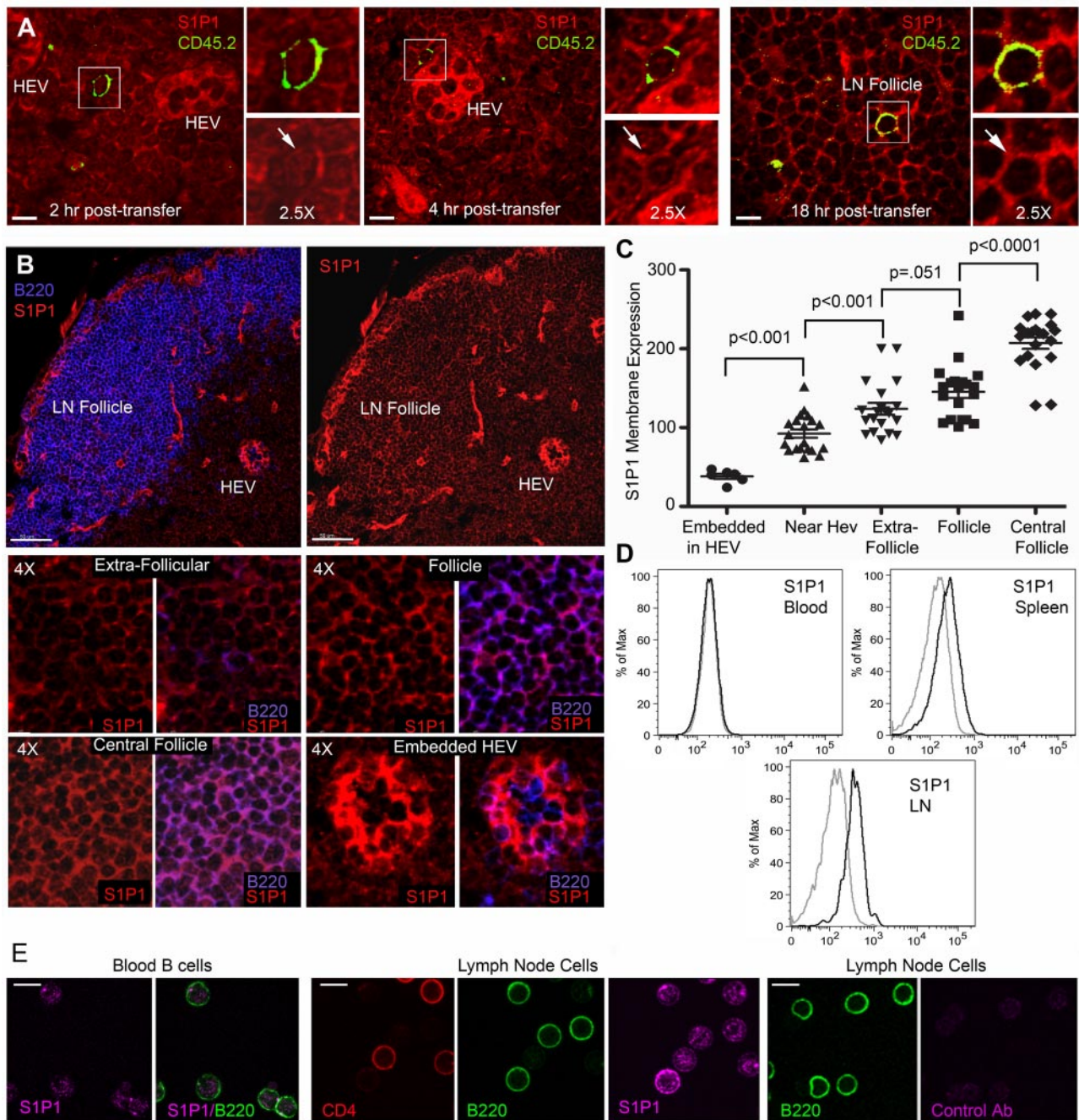
Figure 4. S1P1 receptor expression varies on B cells in the LN. (A) Recently arrived B cells have low S1P1 receptor expression. CD45.2 B cells transferred into CD45.1 mice. LN sections from inguinal LNs of recipient mice were analyzed at 2, 4, and 18 hours after transfer by immunostaining for CD45.2 (green), S1P1 receptor (red), and confocal microscopy. For each condition a composite image is shown to the left along with zoomed (2.5-fold) composite (above) and S1P1 receptor (below) images to the right. S1P1 receptor expression is indicated by an arrow. Similar results were obtained from 2 separate adoptive transfers using 3 recipient mice in each experiment. The strong S1P1 receptor signal arises from the HEV endothelial cells (HEVs). (B) Variation in S1P1 receptor expression at different sites in the LN. Confocal images of LN sections immunostained for B220 (blue) versus S1P1 receptor (red) are shown to the right and S1P1 receptor alone to the left. Scale bars are 50 μm. Eight small images (4× zoom) are shown below from the indicated sites in the LN. Both an S1P1 receptor and a B220/S1P1 receptor image are shown for each location as indicated. (C) Quantification of S1P1 receptor expression. Levels of S1P1 receptor on B cells at various sites in the inguinal LN were quantified by transferring the images to Imaris for analysis of fluorescent intensity. The results are representative of 1 of 4 experiments preformed. Each symbol represents the S1P1 receptor fluorescence of an individual B cell from the indicated sites. Shown are the mean and the standard deviation. The pairwise comparison of adjacent columns was performed using Mann-Whitney test. (D) Flow cytometry of S1P1 receptor expression on blood, spleen, and lymph node B cells. Fixed and permeablized blood, spleen, and lymph node B cells were immunostained for S1P1 expression and analyzed by flow cytometry. Gray line is isotype control. (E) Immunocytochemistry for S1P1 receptor expression on blood and LN B cells. Fixed and permeablized blood cells (first and second panels) were immunostained for B220 (green) and S1P1 receptor (magenta). B220 alone and B220 plus S1P1 are shown. Fixed and permeablized LN cells (third, fourth, and fifth panels) were immunostained for CD4 (red), B220 (green), and S1P1 receptor (magenta). Individual panels are shown. Fixed and permeablized LN cells (sixth and seventh panels) were immunostained for B220 (green) and a control antibody (magenta). Individual panels are shown. All scale bars are 7 μm unless specified otherwise.
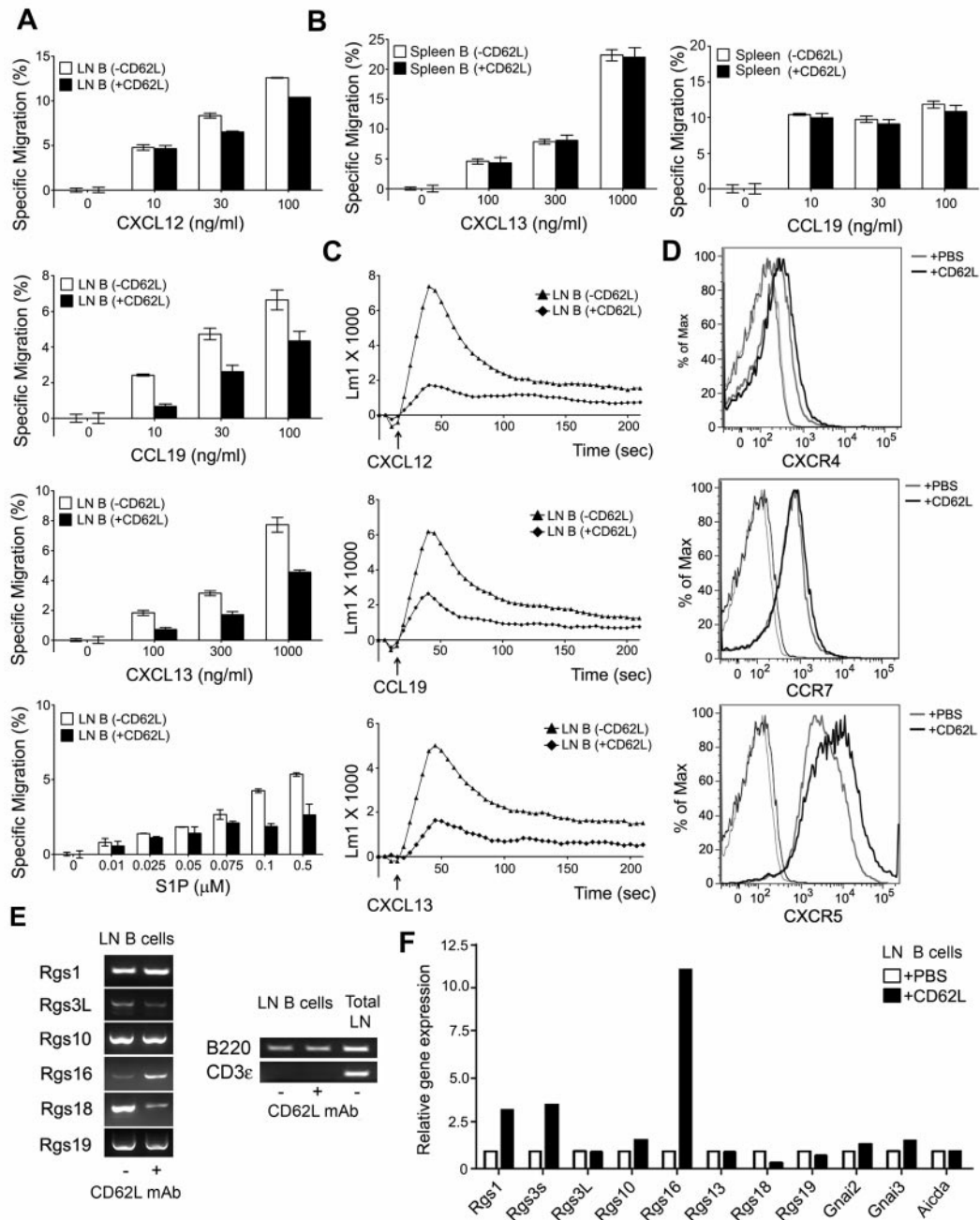
Figure 5. Effect of CD62L antibody treatment on chemokine and S1P1 receptor signaling. (A) LN B cells from CD62L antibody-treated mice exhibit reduced chemotaxis. The experiments shown used B cells prepared from the LNs of 10 CD62L antibody–treated mice (24 hours) and 5 untreated ones. Specific migration to various concentrations of CXCL12, CCL19, CXCL13, and S1P are shown (5 μm pore size). (B) Spleen B cells from CD62L-treated mice respond similar to control spleen cells. Specific migration to various concentrations of CXCL13 and CCL19 is shown. Results are from B cells isolated from 3 treated versus 3 untreated spleens. (C) LN B cells from CD62L antibody-treated mice exhibit reduced chemoattractant induced increases in intracellular calcium. Same B cell preparations were used as in panel A. CXCL12 (100 ng/mL), CCL19 (100 ng/mL), and CXCL13 (100 ng/mL) induced changes in $[Ca^{2+}]_i$ were monitored over 3 minutes, right panels. The data shown as fluorescent counts and the y-axis labeled as Lm1. Each experimental value is the mean of 3 determinations. (D) CD62L antibody treatment does not affect LN B cell chemokine receptor expression. Results shown are from the same LN cells shown in panels A through C. Flow cytometry used to assess CXCR4, CCR7, and CXCR5 expression. Isotype controls are shown at the left of each profile. The chemotaxis, calcium, and flow cytometry were each replicated using smaller numbers of mice. (E-F) CD62L antibody treatment enhances LN B cell RGS protein mRNA expression. Analysis of RNA extracted from same experiment as other panels analyzed by standard RT-PCR (E) and by quantitative RT-PCR (F). The total LN RNA analyzed was prepared from total lymph node lymphocytes and served as a primer control. The quantitative RT-PCR data are shown as relative expression between PBS-treated and CD62L antibody–treated mice.

Blood B cells resensitize their chemokine receptors

After entering the lymph, T and B lymphocytes eventually re-enter the blood. If B cells desensitize their chemoattractant receptors during LN residency, they should reacquire responsiveness to chemokines in the blood. Therefore, we compared the chemokine receptor expression, chemoattractant responses, and chemokine-induced mobilization of intracellular Ca^{2+} between LNs and blood B cells. We found that the blood B cells exhibited a markedly enhanced chemoattractant response compared with LN B cells (Figure 7A). Although the blood B cells expressed more CXCR4 and CCR7 than did LN B cells, CXCR5 and CD62L levels were similar (Figure 7B). Blood B cells mobilized intracellular calcium
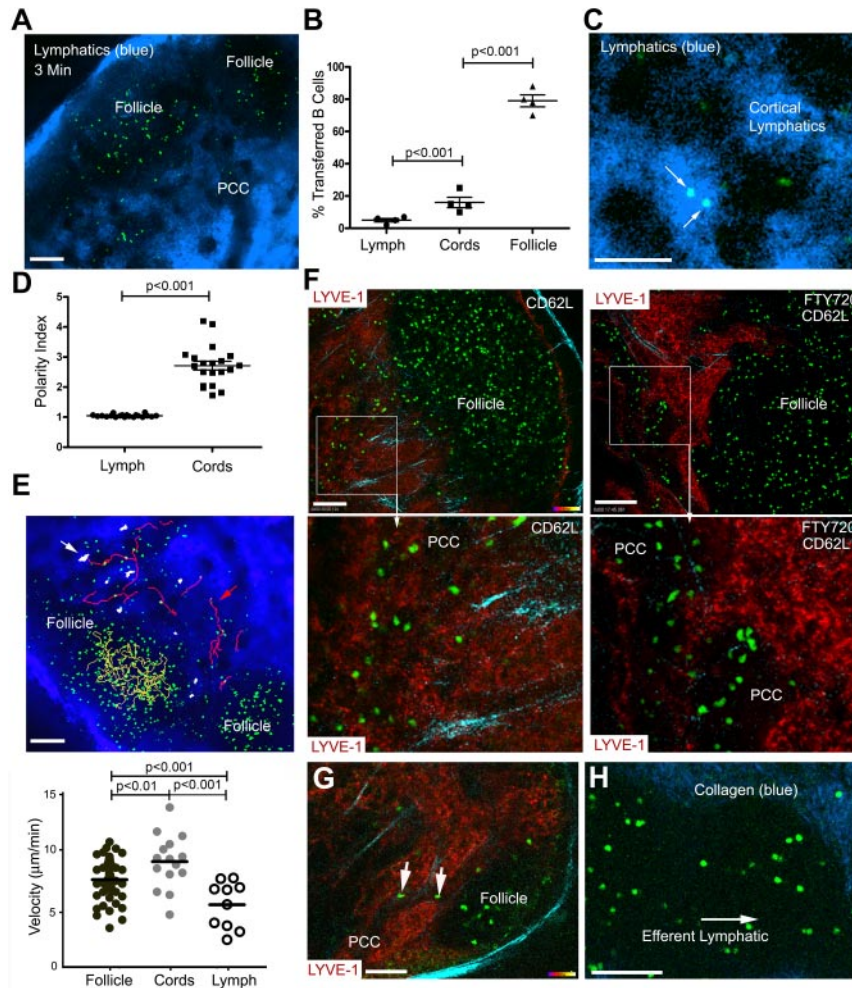
Figure 6. B cells exit the LN follicle into adjacent lymphatics or into the PCCs. (A) Lymphatics outlined by fluorescent nanodots in the lymph. B cells (green) adoptively transferred the day before imaging. Fluorescent nanodots injected subcutaneously near the tail of the recipient 3 minutes before image (single slice) was acquired by TP-LSM. (B) Percentage of transferred B cells in the lymph, PCCs, and LN follicle. The results from the analyses of 4 separate experiments and shown as percentage of total cells in the follicle, PPC, or in the lymph. The image depth from the capsule was approximately 150 μm. (C) Localization of B cells in the lymph. Shown is a TP-LSM image of transferred B cells (green) in the lymph. (D) Polarity index of B cells in the lymph and the PCCs. Polarity index is calculated by dividing the long axis by the short axis of each cell. Individual cells shown. (E) Tracking B cells in the lymph, LN follicle, and PCCs. TP-LSM was used to track and measure the velocity of B cells in the LN follicle (yellow tracks), PCCs (red tracks), and in the lymph (white) of an inguinal LN. The tracks are shown superimposed over an image and individual velocities plotted below. (F) Location of B cells after blocking entrance or blocking entrance and egress. Left images are from TP-LSM of B cells (green, transferred 42 hours earlier) in the LN of a mouse that received CD62L antibody 24 hours after the cell transfer. Lymphatics (red) revealed by injecting labeled LYVE-1 antibody subcutaneously 12 hours before imaging. In the right 2 images the experimental conditions were similar however FTY720 was injected 18 hours after the cell transfer. Bottom images are from outlined regions in the top images. (G) LN B cells exiting the LN follicle into a PCC. A single image is shown from TP-LSM of the inguinal LN that captures 2 B cells (green) exiting into a PCC. LYVE-1 antibody used to reveal the lymphatics. (H) Transferred B cells in a major LN efferent lymphatic. Adoptively transferred B cells (green) flowing in one of the major efferent lymphatics. Collagen is blue. The pair-wise comparisons of indicated columns were performed using Mann-Whitney test. Scale bars are 100 μm.

in response to CXCL13 much better than the LN B cells (Figure 7C). Several RGS proteins were down-regulated in the blood B cells compared with the LN B cells (Figure 7D). Thus, compared with the B cells in the blood, many lymph node B cells express highly desensitized CXCR5, CXCR4, and CCR7 receptors.

Discussion

Similar to 2 recently published TP-LSM investigations of T cells crossing HEVs,[36,37] our observations indicate that after firm adhesion, B cells crawl to explore for intravascular TEM sites. B cells migrated irrespective of the direction of blood flow usually finding a permissive site within 5 minutes of adherence. Once found, the cells moved outside the intravascular lumen within 3 to 5 minutes, whereas T cells needed only a minute. This occurred in

3 stages, the initial protrusion of membrane projections, followed by adoption of an hourglass-like morphology, and the final squeezing of the cell as it crossed the endothelium. Afterward most B cells, but not T cells, remained closely associated with the HEV usually in the perivenule space. This space has been subdivided into 2 channels, the first created by the abluminal side of the endothelial cells and the underlying basement membrane and the second located between the basement membrane and overlying pericytes.[4,38] The lymphocytes observed in the first channel are often flattened, whereas those in the outer channel are more rounded. Our observations are consistent with this description. Shortly after transfer, we easily found poorly motile B cells pancaked along the HEV wall, which subsequently underwent the appearance of a second and occasionally a third TEM. This probably represents the cell pushing through the basement membrane and barriers created by overlapping pericytes. When freed
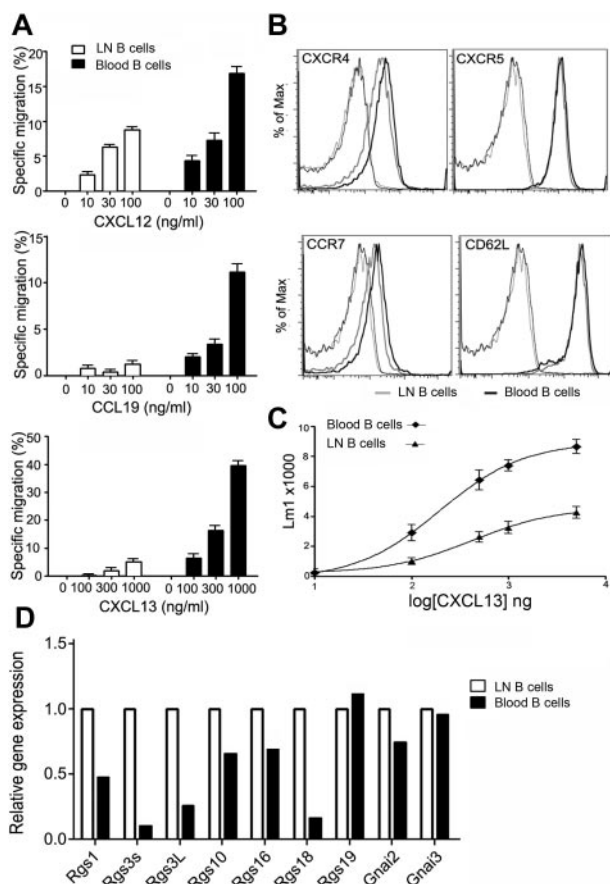
Figure 7. Blood B cells respond better to chemokines and express lower levels of RGS proteins than do LN B cells. (A) Chemotaxis assays. LN and blood B cells were tested in standard chemotaxis assays immediately after isolation. Specific migration to CXCL12, CCL19, and CXCL13 are shown (5-μm pore size). Results are from analysis of negatively selected B cells prepared from pooled LN cells prepared from the inguinal LNs of 6 mice and blood from 15 mice. (B) Comparison of chemokine receptors. Flow cytometry analysis of different chemokine receptors and CD62L on blood and lymph node B cells. Results are from analysis of FACS sorted B cells prepared from pooled LN cells prepared from the inguinal LNs of 6 mice and blood from 15 mice. (C) Comparison of CXCL13 induced changes in $[Ca^{2+}]_i$. CXCL13 induced changes in $[Ca^{2+}]_i$ were monitored over 4 minutes after exposing purified blood or inguinal LN B cells to the indicated concentrations. The data shown as fluorescent counts and the y-axis labeled as Lm1. Each experimental value is the mean of 3 determinations of peak values. The same cells as used in panel B. (D) *Rgs* protein mRNA expression in blood and LN B cells. FACS sorted CD19 and B220 double-positive cells from blood or LN were used to prepare mRNA for quantitative RT-PCR. Each value was normalized to the sample's actin levels and shown as a ratio between the LN and blood B cell value.

from the inner channel, the cell motility increased and they moved parallel or spiral around the HEV, and eventually completed crossing the HEV wall. The retardation of the B cells within the perivenule space may be of physiologic importance because this space is directly connected to the afferent lymph by the conduits.[39,40]

Surprisingly, the *Ccr7−/−* B cells that adhered and crossed HEVs, but had not yet reached the LN follicle, had a motility pattern around the HEVs similar to that of wild-type cells. This argues that there may be another chemoattractant besides CCR7 ligands that supports B-cell motility in this region. Giving further credence to this possibility, the newly emergent B cells that approached the LN follicle failed to enter the follicle, but returned to the HEV area. The apparent retention of cells in this area is of interest as this site is where B cells exiting from HEVs have been shown to interact with dendritic cells bearing cognate antigen.[24] Around 3 to 4 hours after cell transfer, the labeled B cells began to

populate the follicle. The B cells transitioned smoothly into the LN follicle after which they rarely crossed back across the border. During the population of the follicle, the cells entered from underneath gradually accessing the more superficial aspect of the follicle closer to the subcapsular sinus. The behavior of the cells suggests that the cells entered the follicle via the PCCs. The failure of many *Gnai2−/−* B cells to enter the LN follicle and their localization within the interfollicular regions is consistent with the findings examining the localization of *Cxcr5−/−* B cells.[23]

Stimulation of the B cells with LPS before their transfer significantly altered their trafficking pattern. In contrast to the circuitous route followed by nonstimulated B cells, the stimulated cells rapidly crossed HEVs and entered the LN follicle. Although nonstimulated B cells initially avoided the follicle, the stimulated B cells showed no such aversion. This argues that a chemoattractant localized near the HEVs and interfollicular region is affecting the nonstimulated recirculating B cells, whereas the LPS-stimulated cells have probably down-regulated this receptor allowing them to bypass this localizing signal. Because GPR183 facilitates the entrance of B cells into the follicle,[28,29] LPS stimulation may enhance B cell responses to GPR183 ligands promoting the entrance of the activated B cells into the follicle.

The time that B lymphocytes spend in the LN is significantly longer than that of T cells.[41] Eventually B cells leave the LN follicle to enter into the lymph. We show that many LN B cells express chemoattractant receptors poorly responsive to cognate ligand. A reasonable assumption is that the reduction in responsiveness occurs as a function of time spent in the chemokine-rich environment of the LN. This would provide a logical explanation for the reversal of the CXCL13 localizing signal, which would free B cell follicle residents to access cortical lymphatics at the follicle edge or the nearby PCCs. Supporting these ideas we show that those B cells that have resided longer in the LN express higher mRNA levels for RGS proteins. Furthermore, LN B cells respond less well to CCL19 and CXCL13 than do those isolated from spleen or blood. T cells isolated from LN or spleen have been reported to have higher CCR7 occupancy, lower CCR7 expression, and reduced chemotaxis compared with blood T cells.[42]

Although rich in chemokines, the LN parenchyma maintains low S1P levels. B cells in lymphatics and near HEVs express low levels of S1P1 receptor.[10] Using an S1P1 receptor antibody that recognizes an intracellular epitope,[30] we found that LN B cell S1P1 receptors progressively increased as B cells moved away from the HEVs. Furthermore, recently transferred B cells located near HEVs had low levels of S1P1 receptor. This low S1P1 receptor expression on new entrants may explain why the cells do not immediately exit the LN as many HEVs are in close proximity to the cortical lymphatics. As B cells move away from the HEVs into the LN follicle, their increasing levels of S1P1 receptors make them competent for LN egress.

Although decreasing responsiveness to CXCL13 no doubt contributes to B cell egress, a positive signal that recruits B cells to the proximity of egress sites either at the edge of the follicle or in the PCCs is intuitively attractive. An obvious candidate is S1P itself, however, we have found little evidence to support such a role in a previous study[10] and in this study. Other candidates are possible including a GPR183 ligand,[28,29] or an unknown chemoattractant. Either as a consequence of being attracted or random migration, B cells that approach egress sites, a source of S1P, with competent S1P1 receptors receive a signal that promotes their ability to cross from the LN parenchyma into the lymphatics. However, the precise nature of the S1P signal that facilitates

crossing into the lymphatic remains enigmatic. The inability of S1P to provide a transmigration signal for LN B cells in vitro indicates that either the cell line does not provide an adequate model for LN efferent lymphatics or that another signal in addition to S1P is needed. After B cells entered the lymph, they rapidly depolarized. In the course of their journey back into the blood, the B cell chemokine receptors resensitize and CD62L levels rise, increasing the ability of B cells to re-enter secondary lymphoid organs.

In conclusion we have provided a comprehensive evaluation of the trafficking of recirculating B cells through LNs. Although several issues still need resolution, we have proposed a model that is highly dependent on desensitization and resensitization of the functionally important GPCRs (supplemental Figure 4). Although we have assumed that B cells that leave the LN follicle are destined to leave the LN, it remains possible, if not probable, that some B cells return to the PCCs but do not exit, desensitize their S1P receptors or other localizing receptors, and return to the follicle. A complete explanation of the imaging data implies the existence of another chemoattractant receptor-ligand pair that mediates the localization of B cells to the HEV area after their initial entrance. This same receptor-ligand pair could also help relocalize B cells close to egress sites after the exit of B cells from the LN follicle. These studies form the basis for additional studies examining the consequences of antigen stimulation and other perturbations on the trafficking of B lymphocytes.

Authorship

Contribution: C.P. helped design and performed all of the imaging studies and assisted in the chemokine signaling and chemotaxis assays; I.-Y.H. helped design and performed the chemokine signaling and chemotaxis studies; R.K.S. performed the S1P1 receptor immunohistochemistry; O.K. and M.D.D. helped design and perform the S1P studies; and J.H.K. helped design the experiments and wrote the paper.

Conflict-of-interest disclosure: The authors declare no competing financial interests.

Correspondence: Dr John H. Kehrl, NIAID, Bldg 10, Rm 11B08, 9000 Rockville Pike, Bethesda, MD 20892; e-mail: jkehrl@niaid.nih.gov.

References

1. Butcher EC, Picker LJ. Lymphocyte homing and homeostasis. *Science.* 1996;272(5258):60-66.

2. Rosen SD. Ligands for L-selectin: homing, inflammation, and beyond. *Annu Rev Immunol.* 2004; 22:129-156.

3. Shulman Z, Shinder V, Klein E, et al. Lymphocyte crawling and transendothelial migration require chemokine triggering of high-affinity LFA-1 integrin. *Immunity.* 2009;30(3):384-396.

4. Gretz JE, Anderson AO, Shaw S. Cords, channels, corridors and conduits: critical architectural elements facilitating cell interactions in the lymph node cortex. *Immunol Rev.* 1997;156:11-24.

5. Willard-Mack CL. Normal structure, function, and histology of lymph nodes. *Toxicol Pathol.* 2006; 34(5):409-424.

6. Ma B, Jablonska J, Lindenmaier W, Dittmar KE. Immunohistochemical study of the reticular and vascular network of mouse lymph node using vibratome sections. *Acta Histochem.* 2007;109(1): 15-28.

7. Bajenoff M, Egen JG, Koo LY, et al. Stromal cell networks regulate lymphocyte entry, migration, and territoriality in lymph nodes. *Immunity.* 2006; 25(6):989-1001.

8. Forster R, Mattis AE, Kremmer E, Wolf E, Brem G, Lipp M. A putative chemokine receptor, BLR1, directs B cell migration to defined lymphoid organs and specific anatomic compartments of the spleen. *Cell.* 1996;87(6):1037-1047.

9. Reif K, Ekland EH, Ohl L, et al. Balanced responsiveness to chemoattractants from adjacent zones determines B-cell position. *Nature.* 2002; 416(6876):94-99.

10. Sinha RK, Park C, Hwang IY, Davis MD, Kehrl JH. B lymphocytes exit lymph nodes through cortical lymphatic sinusoids by a mechanism independent of sphingosine-1-phosphate-mediated chemotaxis. *Immunity.* 2009;30(3):434-446.

11. Pham TH, Okada T, Matloubian M, Lo CG, Cyster JG. S1P1 receptor signaling overrides retention mediated by G alpha i-coupled receptors to promote T cell egress. *Immunity.* 2008;28(1): 122-133.

12. Mandala S, Hajdu R, Bergstrom J, et al. Alteration of lymphocyte trafficking by sphingosine-1-phosphate receptor agonists. *Science.* 2002; 296(5566):346-349.

13. Matloubian M, Lo CG, Cinamon G, et al. Lymphocyte egress from thymus and peripheral lymphoid organs is dependent on S1P receptor 1. *Nature.* 2004;427(6972):355-360.

14. Lo CG, Xu Y, Proia RL, Cyster JG. Cyclical modulation of sphingosine-1-phosphate receptor 1 surface expression during lymphocyte recirculation and relationship to lymphoid organ transit. *J Exp Med.* 2005;201(2):291-301.

15. Schwab SR, Pereira JP, Matloubian M, Xu Y, Huang Y, Cyster JG. Lymphocyte sequestration through S1P lyase inhibition and disruption of S1P gradients. *Science.* 2005;309(5741):1735-1739.

16. Wei SH, Rosen H, Matheu MP, et al. Sphingosine 1-phosphate type 1 receptor agonism inhibits transendothelial migration of medullary T cells to lymphatic sinuses. *Nat Immunol.* 2005;6(12): 1228-1235.

17. Thangada S, Khanna KM, Blaho VA, et al. Cell-surface residence of sphingosine 1-phosphate receptor 1 on lymphocytes determines lymphocyte egress kinetics. *J Exp Med.* 2010;207(7): 1475-1483.

18. Grigorova IL, Schwab SR, Phan TG, Pham TH, Okada T, Cyster JG. Cortical sinus probing, S1P1-dependent entry and flow-based capture of egressing T cells. *Nat Immunol.* 2009;10(1): 58-65.

19. Rudolph U, Finegold MJ, Rich SS, et al. Ulcerative colitis and adenocarcinoma of the colon in G alpha i2-deficient mice. *Nat Genet.* 1995;10(2): 143-150.

20. Ledgerwood LG, Lal G, Zhang N, et al. The sphingosine 1-phosphate receptor 1 causes tissue retention by inhibiting the entry of peripheral tissue T lymphocytes into afferent lymphatics. *Nat Immunol.* 2008;9(1):42-53.

21. Warnock RA, Askari S, Butcher EC, von Andrian UH. Molecular mechanisms of lymphocyte homing to peripheral lymph nodes. *J Exp Med.* 1998;187(2):205-216.

22. Forster R, Schubel A, Breitfeld D, et al. CCR7 coordinates the primary immune response by establishing functional microenvironments in secondary lymphoid organs. *Cell.* 1999;99(1):23-33.

23. Okada T, Ngo VN, Ekland EH, et al. Chemokine requirements for B cell entry to lymph nodes and Peyer's patches. *J Exp Med.* 2002;196(1):65-75.

24. Qi H, Egen JG, Huang AY, Germain RN. Extrafollicular activation of lymph node B cells by antigen-bearing dendritic cells. *Science.* 2006; 312(5780):1672-1676.

25. Han SB, Moratz C, Huang NN, et al. Rgs1 and Gnai2 regulate the entrance of B lymphocytes into lymph nodes and B cell motility within lymph node follicles. *Immunity.* 2005;22(3):343-354.

26. Hwang IY, Park C, Kehrl JH. Impaired trafficking of Gnai2+/- and Gnai2-/- T lymphocytes: implications for T cell movement within lymph nodes. *J Immunol.* 2007;179(1):439-448.

27. Hwang IY, Park C, Harrison K, Kehrl JH. TLR4 signaling augments B lymphocyte migration and overcomes the restriction that limits access to germinal center dark zones. *J Exp Med.* 2009; 206(12):2641-2657.

28. Gatto D, Paus D, Basten A, Mackay CR, Brink R. Guidance of B cells by the orphan G protein-coupled receptor EBI2 shapes humoral immune responses. *Immunity.* 2009;31(2):259-269.

29. Pereira JP, Kelly LM, Xu Y, Cyster JG. EBI2 mediates B cell segregation between the outer and centre follicle. *Nature.* 2009;460(7259):1122-1126.

30. Akiyama T, Sadahira Y, Matsubara K, Mori M, Igarashi Y. Immunohistochemical detection of sphingosine-1-phosphate receptor 1 in vascular and lymphatic endothelial cells. *J Mol Histol.* 2008;39(5):527-533.

31. Cho H, Kehrl JH. Regulation of immune function by G protein-coupled receptors, trimeric G proteins, and RGS proteins. *Prog Mol Biol Transl Sci.* 2009;86:249-298.

32. Hwang IY, Park C, Harrision KA, Huang NN, Kehrl JH. Variations in Gnai2 and Rgs1 expression affect chemokine receptor signaling and the organization of secondary lymphoid organs. *Genes Immun.* 2010;11(5):384-396.

33. Kelly E, Bailey CP, Henderson G. Agonist-selective mechanisms of GPCR desensitization. *Br J Pharmacol.* 2008;153(Suppl 1):S379-S388.

34. Donovan EE, Pelanda R, Torres RM. S1P3 confers differential S1P-induced migration by autoreactive and non-autoreactive immature B cells and is required for normal B-cell development. *Eur J Immunol.* 2010;40(3):688-968.

35. Allende ML, Tuymetova G, Lee BG, Bonifacino E, Wu YP, Proia RL. S1P1 receptor directs the release of immature B cells from bone marrow into blood. *J Exp Med.* 2010;207(5):1113-1124.

36. Park EJ, Peixoto A, Imai Y, et al. Distinct roles for LFA-1 affinity regulation during T-cell adhesion, diapedesis, and interstitial migration in lymph nodes. *Blood.* 2010;115(8):1572-1581.

37. Boscacci RT, Pfeiffer F, Gollmer K, et al. Comprehensive analysis of lymph node stroma-expressed Ig superfamily members reveals redundant and nonredundant roles for ICAM-1, ICAM-2, and VCAM-1 in lymphocyte homing. *Blood.* 2010;116(6):915-925.

38. Nourshargh S, Hordijk PL, Sixt M. Breaching multiple barriers: leukocyte motility through venular walls and the interstitium. *Nat Rev Mol Cell Biol.* 2010;11(5):366-378.

39. Gretz JE, Norbury CC, Anderson AO, Proudfoot AE, Shaw S. Lymph-borne chemokines and other low molecular weight molecules reach high endothelial venules via specialized conduits while a functional barrier limits access to the lymphocyte microenvironments in lymph node cortex. *J Exp Med.* 2000;192(10):1425-1440.

40. Sixt M, Kanazawa N, Selg M, et al. The conduit system transports soluble antigens from the afferent lymph to resident dendritic cells in the T cell area of the lymph node. *Immunity.* 2005;22(1):19-29.

41. Tomura M, Yoshida N, Tanaka J, et al. Monitoring cellular movement in vivo with photoconvertible fluorescence protein "Kaede" transgenic mice. *Proc Natl Acad Sci U S A.* 2008;105(31):10871-10876.

42. Britschgi MR, Link A, Lissandrin TK, Luther SA. Dynamic modulation of CCR7 expression and function on naive T lymphocytes in vivo. *J Immunol.* 2008;181(11):7681-7688.